BPM Button Characterization for Offset Calibration

Y. Chung

March, 1992

Abstract

In this note, a basic theory of wave propagation in dielectric media is discussed in conjunction with S parameters to derive the button gain coefficient g_e and an analytic expression for the signal from time domain reflectometry (TDR) measurement on a cable and a button. The results can be used to measure the button capacitance and the characteristic impedances of the cable and the button feedthrough. Since g_e is a function of S parameters and the button capacitance C_p, a suggestion is made to make the gain coefficients the same for all four buttons in a BPM by carefully matching the buttons and the cables.

1. Introduction

In order to achieve the stringent performance specifications for the beam position monitors (BPMs) in the APS storage ring as shown in Table 1.1, it is necessary to calibrate the offset and the sensitivity of all BPMs with an accuracy of less than 30 μm in both the horizontal and the vertical directions. Because the BPM is an integral part of the vacuum chamber (≈ 5 m long), it will be very difficult to calibrate the BPMs using wire suspended inside the vacuum chamber.

The external calibration method developed by G. Lambertson[1-4] requires only measurements of coupling between two sets of buttons and cables using a network analyzer. With four buttons for each BPM, 12 such measurements are needed, from which are derived the four gain coefficients associated with each set of a button and a cable. In Lambertson's theory[1], the gain coefficient g_e was expressed as

$$g_e = \frac{S_{12}}{1 - S_{11}}. \tag{1.1}$$

S_{11} is the reflection coefficient on the feedthrough's side for the combination of all cables, connectors, and the feedthrough, and S_{12} is the transmission coefficient for either direction.

The gain coefficient g_e is a function of frequency and Eq. (1.1) is valid when the frequency is low enough. With a button capacitance C_p and characteristic impedance Z_0, the relevant time scale is C_pZ_0. Therefore, when ωC_pZ_0 is comparable to or larger than 1, more rigorous treatment is needed in deriving the gain coefficient. For the APS beam position monitoring system the signal detection is done at the fundamental RF frequency of 351.92 MHz and typical button capacitance is 5 pF, which gives $\omega C_pZ_0 = 0.553$.

First Turn, 1 mA Resolution / Accuracy	200 μm / 500 μm
Stored Beam, Single or Multiple Bunches @ 5mA Total Resolution / Accuracy	25 μm / 200 μm
Stability, Long Term	±30 μm
Dynamic Range, Intensity	≥ 40 dB
Dynamic Range, Position	±20 mm

Table 1.1: APS Storage Ring Beam Position Monitor Specifications.

In the following sections we will first discuss the problem of wave propagation in multiple dielectric media, e.g., cables, connectors, and feedthroughs. Coefficients of reflection and transmission will be derived in conjunction with S parameters. Then a more generalized theory will be developed for calibrating the electrical offset using external means which takes into account the effect of finite button capacitance. We will also discuss use of time domain reflectometry (TDR) to determine the button capacitance and the characteristic impedances of cables and feedthroughs. If these can be accurately measured, buttons and cables can be sorted and matched in such a manner that the gain coefficients for the four buttons are nearly identical, whereby the electrical offset becomes negligibly small. A summary of this article will be presented in the last section.

2. Wave Propagation in Multiple Media

In this section, we will treat propagation of voltage and current waves in dielectric media, such as cables, connectors, and button feedthroughs.

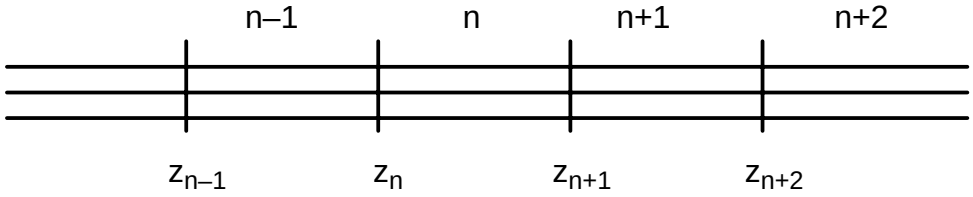

Fig. 2.1: Multiple waveguides connected in series. The n-th cable, with the characteristic impedance of Z_n, starts at $z = z_n$ and ends at $z = z_{n+1}$.

Consider multiple cables connected in series as shown in Fig. 2.1. We assume that there are total of m such cables. The n-th cable, with the characteristic impedance of Z_n, starts at $z = z_n$ and ends at $z = z_{n+1}$. Let V(z,t) and I(z,t) be the voltage and the current at point z and at time t. With the series resistance R_n, the series inductance L_n, the conductance G_n, and the shunt capacity C_n, the voltage and current satisfy the relations[5]

$$\frac{\partial V}{\partial z} = -R_n I - L_n \frac{\partial I}{\partial t}, \quad \frac{\partial I}{\partial z} = -G_n V - C_n \frac{\partial V}{\partial t}, \quad (n = 1, \ldots, m) \tag{2.1}$$

in the n-th cable. In the following discussion, we will ignore R_n and G_n and consider only dispersionless and lossless cables. L_n and C_n are given as

$$L_n = \frac{\mu n}{2\pi} \log \frac{b_n}{a_n}, \quad C_n = \frac{2\pi\varepsilon_n}{\log \frac{b_n}{a_n}}. \tag{2.2}$$

a_n and b_n are the radii of the inner and the outer conductors in the cable. Thus we have

$$\frac{\partial V}{\partial z} = -L_n \frac{\partial I}{\partial t}, \quad \frac{\partial I}{\partial z} = -C_n \frac{\partial V}{\partial t}. \qquad (n = 1, ..., m) \tag{2.3}$$

There are a couple of techniques to solve Eq. (2.3). In this section we will consider the case of continuous wave, and apply Fourier transform to obtain the reflection and transmission coefficients. A different method involving Laplace transform will be used later to solve the problem of TDR.

Combining the two equations in Eq. (2.3), we obtain

$$\frac{\partial^2 V}{\partial z^2} - \frac{1}{v_n{}^2} = \frac{\partial^2 V}{\partial t^2} = 0, \qquad (z_n < z < z_{n+1}) \tag{2.4}$$

where $v_n = 1/\sqrt{L_n C_n}$. Write the voltage wave V(z,t) as

$$V(z,t) = \int_{-\infty}^{\infty} dk \, \{A_n(k)e^{ik(z-z_n)} + B_n(k)e^{-ik(z-z_n)}\}e^{-ikn_v t}. \quad (z_n < z < z_{n+1}) \tag{2.5}$$

Then from Eq. (2.3), we have the current I(z,t) as

$$I(z,t) = \frac{1}{Z_n} \int_{-\infty}^{\infty} dk \, \{A_n(k)e^{ik(z-z_n)} - B_n(k)e^{-ik(z-z_n)}\}e^{-ikn_v t}. \quad (z_n < z < z_{n+1}) \tag{2.6}$$

where $Z_n = \sqrt{L_n/C_n}$ is the characteristic impedance of the n-th cable. The first terms in Eqs. (2.5) and (2.6) represent the forward-traveling wave and the second terms represent the backward-traveling wave. The ratio $R_n(k) = B_n(k) / A_n(k)$ is the reflection coefficient in the n-th cable. The continuity of V(z,t) and I(z,t) at the boundary between the n-th and the (n+1)-th cables gives

$$A_{n+1} + B_{n+1} = A_n e^{ikl_n} + B_n e^{-ikl_n}. \tag{2.7}$$

$$\frac{1}{Z_{n+1}} (A_{n+1} - B_{n+1}) = \frac{1}{Z_n} (A_n e^{ikl_n} - B_n e^{-ikl_n}). \tag{2.8}$$

From Eqs. (2.7) and (2.8), with $R_n = B_n / A_n$,

$$Z_n \frac{1 + R_n e^{-2ikl_n}}{1 - R_n e^{-2ikl_n}} = Z_{n+1} \frac{1 + R_{n+1}}{1 - R_{n+1}}. \tag{2.9}$$

or,

$$R_n = e^{2ikl_n} \frac{\frac{Z_{n+1}}{Z_n} \frac{1+R_{n+1}}{1-R_{n+1}} - 1}{\frac{Z_{n+1}}{Z_n} \frac{1+R_{n+1}}{1-R_{n+1}} + 1}. \tag{2.10}$$

$l_n = z_{n+1} - z_n$ is the length of the n-th cable. Equation (2.10) is the recursion relation for finding R_n once the reflection coefficient in the last cable (n = m) is known. This procedure will determine the reflection coefficients in all the cables. From Eq. (2.7),

$$A_{n+1} = \frac{1 + R_n e^{-2ikl_n}}{1 + R_{n+1}} e^{ikl_n} A_n$$

$$= \left(\frac{1 + R_n e^{-2ikl_n}}{1 + R_{n+1}}\right) \left(\frac{1 + R_{n-1} e^{-2ikl_n}}{1 + R_n}\right) ... \left(\frac{1 + R_1 e^{-2ikl_1}}{1 + R_2}\right) e^{ik\Sigma l_n} A_1, \tag{2.11}$$

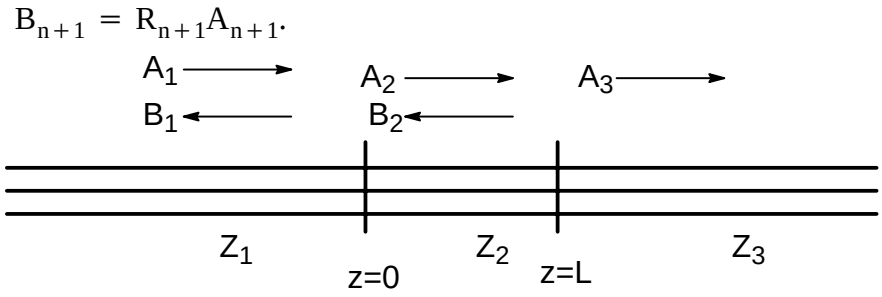

Fig. 2.2: Three cables connected in series. The third cable is terminated so that there is no backward-traveling wave. l_1 is taken to be zero.

Consider an example of three cables connected in series as shown in Fig. 2.2. Since it is assumed that there is no reflected wave in cable 3, we put $R_3 = 0$. Using Eq. (2.10), we have

$$R_2 = e^{2ikL}\frac{Z_3 - Z_2}{Z_3 + Z_2},$$

$$R_1 = \frac{\frac{Z_2}{Z_1}\frac{Z_3 - iZ_2\tan(kL)}{Z_2 - iZ_3\tan(kL)} - 1}{\frac{Z_2}{Z_1}\frac{Z_3 - iZ_2\tan(kL)}{Z_2 - iZ_3\tan(kL)} + 1}. \tag{2.12}$$

3. S parameters

Consider a cable of length L and characteristic impedance Z_c. We want to calculate the S parameters of this cable attached to cables with the characteristic impedance Z_T as shown in Fig. 3.1. It is assumed that the instrument ports are properly terminated with resistors Z_T so that there is no reflection.

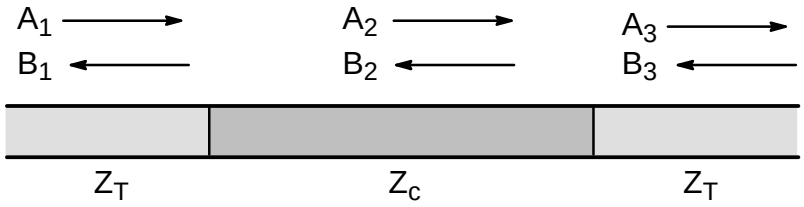

Fig. 3.1: Forward- and backward-traveling waves in a cable for S parameter measurement.

The A_n and B_n coefficients are related to each other through the S parameters:

$$\begin{pmatrix} B_1 \\ A_3 \end{pmatrix} = \begin{pmatrix} S_{11} & S_{12} \\ S_{21} & S_{22} \end{pmatrix} \begin{pmatrix} A_1 \\ B_3 \end{pmatrix}. \tag{3.1}$$

The S parameters are

$$S_{11} = \left(\frac{B_1}{A_1}\right)_{B_3=0}, \; S_{12} = \left(\frac{B_1}{B_3}\right)_{A_1=0}, \; S_{21} = \left(\frac{A_3}{A_1}\right)_{B_3=0} \text{ and } S_{22} = \left(\frac{A_3}{B_3}\right)_{A_1=0}. \tag{3.2}$$

This is the same situation as in Fig. 2.2 and S_{11} is the same as R_1 in Eq. (2.12). The transmission coefficient S_{12} can be obtained using Eq. (2.11). With $Z_1 = Z_3 = Z_T$, $Z_2 = Z_c$ and after some rearrangement, we obtain[6]

$$S_{11} = S_{22} = \frac{-i(Z_{c^2} - Z_{T^2})\tan(kL)}{2Z_cZ_T - i(Z_{c^2} + Z_{T^2})\tan(kL)}, \tag{3.3}$$

$$S_{12} = S_{21} = \frac{2 \sec (kL)\ Z_c Z_T}{2\ Z_c Z_T - i(Z_{c^2} + Z_{T^2}) \tan (kL)}, \tag{3.4}$$

for a single cable with characteristic impedance Z_c.

Once the S parameters for a single cable are obtained, we can extend the calculation to multiple cables connected in series. Consider two sets of cables a and b, each comprising multiple cables. Let S^a and S^b be the corresponding S matrices and let S be the S matrix of the total system combining a and b. Then it can be shown that (see Appendix A)

$$S_{11} = S^a_{11} = \frac{S^a_{12} S^a_{21} S^b_{11}}{1 - S^a_{22} S^b_{11}}, \tag{3.5}$$

$$S_{12} = \frac{S^a_{12} S^b_{12}}{1 - S^a_{22} S^b_{11}}, \tag{3.6}$$

$$S_{21} = \frac{S^a_{21} S^b_{21}}{1 - S^a_{22} S^b_{11}}, \tag{3.7}$$

$$S_{22} = S^b_{22} = \frac{S^a_{22} S^b_{21} S^b_{12}}{1 - S^a_{22} S^b_{11}}. \tag{3.8}$$

Equations (3.6) and (3.7) show that if $S^a_{12} = S^a_{21}$ and $S^b_{12} = S^b_{21}$, then we have

$$S_{12} = S_{21}. \tag{3.9}$$

Since this is the case with a single cable, it is also true for any number of cables connected in series.

4. Button Gain Coefficients

In this section we will derive the button gain coefficient g_e for a given current source in terms of the S parameters. A current source can be a charged particle beam, a wire, or a button driven by an RF source, which induces a flow of charges through electromagnetic coupling. Since the button has a finite capacitance C_p, some of the current flows through the capacitor to the ground and some flows through the cables and a terminating resistor at the end. This is shown in Fig. 4.1(a). Let I' be the current through the capacitor and let I be the current through the cables. Then, assuming harmonic time dependence $e^{-i\omega t}$, we have $I = I_0 - I' = I_0 + i\omega C_p V$, which gives

$$A_1 = I_0 Z_1 \frac{1}{1 - R_1 - i\omega C_p Z_1 (1 + R_1)}. \tag{4.1}$$

This is the boundary condition at z = 0. On the other side of the cable we have $V = Z_T I$, which gives

$$R_m = e^{2ikl_m} \frac{Z_T - Z_m}{Z_T + Z_m}. \tag{4.2}$$

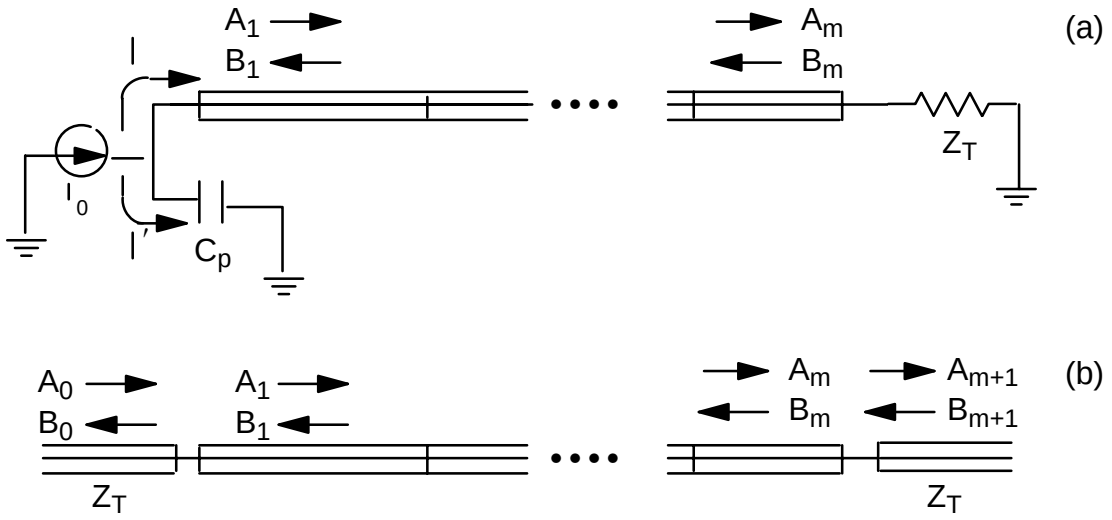

Fig. 4.1: (a) Button signal detection with current source I_0.
(b) S parameter measurement setup simulating the button signal measurement.

Eqs. (4.1) and (4.2) are the two necessary conditions to completely determine the A_n and B_n coefficients in all the individual components.

In order to express the detected signal in terms of the S parameters, let us consider the setup in Fig. 4.1(b). This simulates the setup in Fig. 4.1(a) by correctly setting the input voltage level A_0. The coefficients A_0, B_0, A_{m+1}, and B_{m+1} are related to each other by

$$\begin{pmatrix} B_0 \\ A_{m+1} \end{pmatrix} = \begin{pmatrix} S_{11} & S_{12} \\ S_{21} & S_{22} \end{pmatrix} \begin{pmatrix} A_0 \\ B_{m+1} \end{pmatrix}. \tag{4.3}$$

Since there is no reflection from the right side, we put $B_{m+1} = 0$. From Eq. (2.11) the coefficient A_{m+1} can be written

$$\begin{aligned} A_{m+1} &= e^{ik\Sigma l_n} \left(\frac{1 + R_m e^{-2ikl_m}}{1 + R_{m+1}} \right) \left(\frac{1 + R_{m-1} e^{-2ikl_{m-1}}}{1 + R_m} \right) \cdots \left(\frac{1 + R_0}{1 + R_1} \right) A_0 \\ &= S_{21} A_0, \end{aligned} \tag{4.4}$$

which is the detected signal at the end of the cable. With

$$A_0 = A_1 \left(\frac{1 + R_1}{1 + R_0} \right), \tag{4.5}$$

and the desired coefficient A_1 given by Eq. (4.1), the input amplitude A_0 is set to

$$A_0 = \frac{I_0 Z_1}{1 + S_{11} \frac{1 - R_1}{1 + R_1} - i\omega C_p Z_1}. \tag{4.6}$$

where we used $S_{11} = R_0$. Also, from Eq. (2.9), we have

$$\frac{1 - R_1}{1 + R_1} = \frac{Z_1}{Z_T} \frac{1 - S_{11}}{1 + S_{11}}. \tag{4.7}$$

Combining Eqs. (4.4), (4.6), and (4.7), we obtain the detected signal V_d

$$V_d = A_{m+1} = g_e I_0 Z_T, \tag{4.8}$$

where

$$g_e = \frac{S_{21}}{1 - S_{11} - i\omega C_p Z_T(1 + S_{11})}. \tag{4.9}$$

This is the expression for the button gain coefficient that relates the induced current on the electrode and the detected voltage. Typically, $|S_{11}| << 1$ and $|S_{21}| \approx 1$, and in the limiting case where $S_{11} = 0$ and $S_{21} = 1$, $g_e Z_T$ reduces to

$$g_e Z_T = \left(\frac{1}{Z_t} - i\omega C_p\right)^{-1}. \tag{4.10}$$

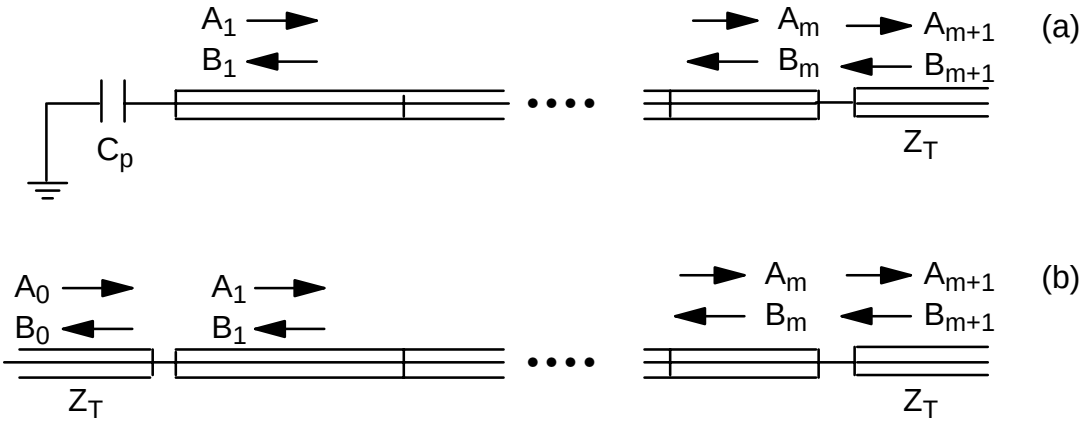

Fig. 4.2: (a) A button driven externally by an RF source.
(b) S parameter measurement setup to simulate driving the button externally.

Next, consider driving a button externally using an RF source. The schematic is shown in Fig. 4.2(a). We use an approach similar to that described in the previous paragraph to express the voltage on the button in terms of the S parameters.

The boundary condition at the capacitance is $V = \frac{I}{i\omega C_p}$, which gives

$$\frac{1 + R_1}{1 - R_1} = \frac{1}{i\omega C_p Z_1}. \tag{4.11}$$

From this relationship and and from Eq. (2.10), we obtain

$$R_0 = \frac{\frac{Z_1}{Z_T}\frac{1+R_1}{1-R_1} - 1}{\frac{Z_1}{Z_T}\frac{1+R_1}{1-R_1} + 1} = \frac{1 - i\omega C_p Z_T}{1 + i\omega C_p Z_T}. \tag{4.12}$$

From Eq. (4.3), we have $B_0 = S_{11}A_0 + S_{12}B_{m+1}$, which gives

$$B_0 = \frac{S_{12}R_0}{R_0 - S_{11}} B_{m+1}. \tag{4.13}$$

Let V_e be the voltage on the electrode and let $V_s = B_{m+1}$ be the driving voltage at the RF source. Then using Eqs. (4.12) and (4.13), we have

$$V_e = A_{0+}B_0$$

$$= \frac{2S_{21}}{1 - S_{11} - i\omega C_p Z_T(1 + S_{11})} V_S \tag{4.14}$$
$$= g_e V_s,$$

when $S_{12} = S_{21}$. Noted that the gain coefficient g_e is the same as in Eq. (4.9).

5. Time Domain Reflectometry of Buttons

In this section, we will consider TDR measurement on buttons. This technique can be used to determine the S parameters of the cable and the button feedthrough by measuring the cable length and the characteristic impedances and using Eqs. (3.3) and (3.4).

5.1 Theory

Taking the Laplace transform of Eq. (2.3), we obtain

$$\frac{\partial \tilde{V}(z,s)}{\partial z} + L_n(s\tilde{I}(z,s) - I(z,0)) = 0, \tag{5.1}$$

$$\frac{\partial \tilde{I}(z,s)}{\partial z} + C_n(s\tilde{V}(z,s) - V(z,0)) = 0, \tag{5.2}$$

where s is the Laplace transform variable. Equations (5.1) and (5.2), together with the proper boundary conditions, completely describe the system, and solutions for the voltage and current can be obtained for all times $t > 0$ for given initial conditions V(z,0) and I(z,0). Combining Eqs. (5.1) and (5.2) gives

$$\frac{\partial^2 \tilde{V}}{\partial z^2} - L_n C_n s^2 \tilde{V} = - L_n C_n s V(z,0), \tag{5.3}$$

whose solution is (see Appendix B)

$$\tilde{V}(z,s) = A'_n e^{-h_n z} + B'_n e^{h_n z} + \frac{h_n}{2s} \int_{-\infty}^{\infty} dz' \; e^{h_n|z-z'|}\left(v(z',0) + \frac{1}{s}\frac{\partial V}{\partial t}(z',0)\right), \tag{5.4}$$

where $h_n = s\sqrt{L_n C_n}$ and A'_n and B'_n are functions of s yet to be determined. A similar solution can be obtained for the current, which is

$$\tilde{I}(z,s) = \frac{1}{Z_n}(A'_n e^{-h_n z} - B'_n e^{h_n z}) + \frac{h_n}{2s} \int_{-\infty}^{\infty} dz' \; e^{h_n|z-z'|}\left(I(z',0) + \frac{1}{s}\frac{\partial I}{\partial t}(z'0)\right), \tag{5.5}$$

where $Z_n = \sqrt{L_n/C_n}$ is the characteristic impedance of the n-th cable. The initial values for current I(z′,0) and $\frac{\partial I}{\partial t}(z',0)$ can be found from the initial values for voltage V(z′,0) and $\frac{\partial V}{\partial t}(z',0)$ using Eq. (2.3).

As an example, suppose the initial conditions are

$$V(z,0) = V_0, \qquad \text{in the cables,}$$
$$\frac{\partial V}{\partial t}(z,0) = 0. \qquad \text{for all z.} \tag{5.6}$$

V_0 is the initial constant voltage level at t = 0. Inserting Eq. (5.6) into Eqs. (5.4) and (5.5), we can rewrite $\tilde{V}(z, s)$ and $\tilde{I}(z,s)$ as

$$\tilde{V}(z, s) = A_n e^{-h_n(z-z_n)} + B_n e^{h_n(z-z_n)} + \frac{V_0}{s}, \tag{5.7}$$

$$\tilde{I}(z, s) = \frac{1}{Z_n}\left\{A_n e^{-h_n(z-z_n)} - B_n e^{h_n(z-z_n)}\right\}. \tag{5.8}$$

A_n and B_n are new constants, into which were absorbed parts of the integral. Assuming harmonic time dependence $e^{-i\omega t}$, the first terms in Eqs. (5.7) and (5.8) represent the forward-traveling wave and the second terms represent the backward-traveling wave. The ratio $R_n = B_n / A_n$ is the reflection coefficient in the n-th cable. The continuity of $\tilde{V}$ and $\tilde{I}$ at the boundary between the n-th and the (n+1)-th cables gives a relation analogous to Eq. (2.9)

$$Z_n = \frac{1 + R_n e^{2h_n 1_n}}{1 - R_k e^{2h_n l_n}} = Z_{n+1}\frac{1 + R_{n+1}}{1 - R_{n+1}}, \tag{5.9}$$

or,

$$R_n = e^{-2h_n l_n}\frac{\frac{Z_{n+1}}{Z_n}\frac{1+R_{n+1}}{1-R_{n+1}} - 1}{\frac{Z_{n+1}}{Z_n}\frac{1+R_{n+1}}{1-R_{n+1}} + 1}. \tag{5.10}$$

$l_n = z_{n+1} - z_n$ is the length of the n-th cable. Eq. (5.10) is the recursion relation for finding R_n once the reflection coefficient in the last cable (n = m) is known. This procedure will determine the reflection coefficients in all the cables. With an additional boundary condition in the first cable (n = 1) giving the relation between A_1 and B_1, the problem is solved in principle.

5.2 TDR of an Open-Ended Cable

Let us take an example of an open-ended cable to apply the technique of TDR to measure the length l and the characteristic impedance Z_c. The schematic of this TDR measurement is shown in Fig. 5.1. The measurement instrument has a variable current source which is connected to the terminating resistor Z_T. Then a step pulse is generated when the current source is switched off. This pulse propagates out to the external device and the signal at the acquisition point is detected as a function of time.

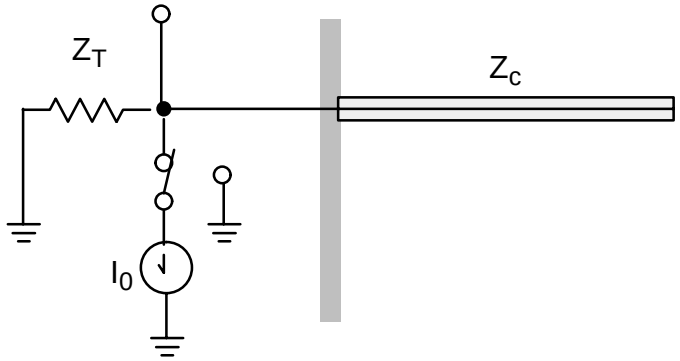

Fig. 5.1: The schematic of the time domain reflectometry measurement of an open-ended cable of length l. When t < 0, the switch at the current source is closed. At t = 0, the switch opens and the propagation of the voltage change begins to propagate to the right.

We apply the results obtained in Section 5.1 with the boundary conditions

$$V(0,t) = -Z_T I(0,t) \tag{5.11}$$

and

$$I(l,t) = 0. \tag{5.12}$$

Taking the Laplace transform of Eqs. (5.11) and (5.12), we have

$$\tilde{V}(0,s) = -Z_T \tilde{I}(0,s), \tag{5.13}$$

$$\tilde{I}(l,s) = 0. \tag{5.14}$$

These two boundary conditions and Eqs. (5.7), (5.8), and (5.10) determine the coefficients A_1 and B_1, which are given by

$$A_1 = \frac{I_0 Z_T Z_C}{Z_T + Z_c}\frac{1}{s}\frac{1}{1 - r\, e^{-2s\Delta t}}, \tag{5.15}$$

and

$$B_1 = \frac{I_0 Z_T Z_c}{Z_T + Z_c}\frac{1}{s}\frac{e^{-2s\Delta t}}{1 - r\, e^{-2s\Delta t}}, \tag{5.16}$$

where

$$\Delta t = \frac{1}{v}, \quad v = \frac{1}{\sqrt{LC}}, \quad \text{and} \quad r = \frac{Z_T - Z_c}{Z_T + Z_c}. \tag{5.17}$$

v is the wave propagation velocity in the cable, r is the impedance mismatch ratio and Δt is the time taken to propagate through the length of the cable. Substituting Eqs. (5.15) and (5.16) into Eq. (5.7), we get

$$\tilde{V}(z,s) = \frac{I_0 Z_T}{s}\left\{\frac{Z_C}{Z_T + Z_c}\frac{e^{-sz/v} + e^{s(z-2\Delta t)/v}}{1 - r\, e^{-2s\Delta t}} - 1\right\}. \tag{5.18}$$

The desired voltage function V(z,t) can be obtained by doing the inverse-Laplace transform of Eq. (5.18). Since this cannot be done in a closed form, we expand $\tilde{V}(z,s)$ into a series by noting that $|r|\, e^{-2s\Delta t}$ is always less than 1. The result is

$$\tilde{V}(z,s) = \frac{I_0 Z_T}{s}\left[\frac{Z_c}{Z_T + Z_c}\left\{e^{-sz/v} + e^{s(z/v - 2\Delta t)}\right\}\sum_{n=0}^{\infty} r^{-2ns\Delta t} - 1\right]. \tag{5.19}$$

Now, from the relationship

$$e^{-\beta s}\tilde{f}(s) \xrightarrow{\text{Inverse - Laplace}} f(t - \beta), \tag{5.20}$$

the n-th term in the summation of Eq. (5.18) corresponds to time delay of $2n\Delta t$ and attenuation of r^n. The time evolution of voltage V(z,t) is then the result of multiple reflections and transmissions at the boundaries at z = 0 and z = l, which rapidly decays to zero when the impedance is closely matched ($|r| << 1$). The detected signal V(0,t) is then obtained from

$$\tilde{V}(0,s) = -\frac{I_0 Z_{T^2}}{Z_T + Z_c}\frac{1}{s}\left\{1 - \frac{2Z_C}{Z_T + Z_c}\sum_{n=1}^{\infty} r^{n-1} e^{-2ns\Delta t}\right\}. \tag{5.21}$$

Since the inverse-Laplace transform of $\frac{1}{s}$ is the unit step function u(t) given by

$$u(t) = \begin{cases} 0, & t < 0 \\ 1/2, & t = 0 \\ 1, & t \geq 0 \end{cases} \tag{5.22}$$

we have

$$V(0,t) = -\frac{I_0 Z_{T^2}}{Z_T + Z_c}\left\{u(t) - \frac{2Z_c}{2_T + Z_c}\sum_{n=1}^{\infty} r^{n-1}U(t - 2n\Delta t)\right\}. \qquad (t > 0) \tag{5.23}$$

When the impedance is matched ($Z_c = Z_T$), V(0,t) = 0 for $t > 2\Delta t$. Otherwise, there are discontinuities in the signal at every $2\Delta t$. Figure 5.2 shows a sample TDR signal of an open-ended cable with $Z_T = 50\ \Omega$, $Z_c = 100\ \Omega$, and $I_0 = 10$ mA. For $0 < t < 2\Delta t$, the signal level is constant at

$$V(0,t) = -\frac{I_0 Z_{T^2}}{Z_T + Z_c}. \qquad (0 < t < 2\Delta t) \tag{5.24}$$

Equation (5.24) can be used to determine the characteristic impedance and the length of a cable by measuring the signal level and the time duration.

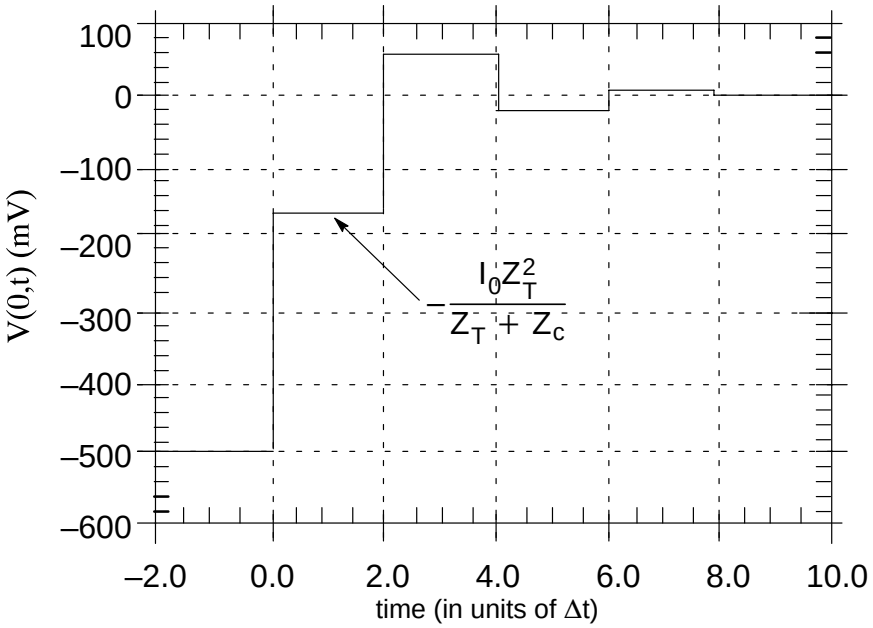

Fig. 5.2: Theoretically derived TDR trace of an open-ended cable, with $Z_T = 50\Omega$, $Z_c = 100\Omega$, and $I_0 = 10$ mA.

5.3 TDR of a Button

We now consider application of TDR to the measurement of the capacitance of the button and the characteristic impedances of the button feedthrough and the connecting cable. The schematic of the TDR measurement is shown in Fig. 5.3.

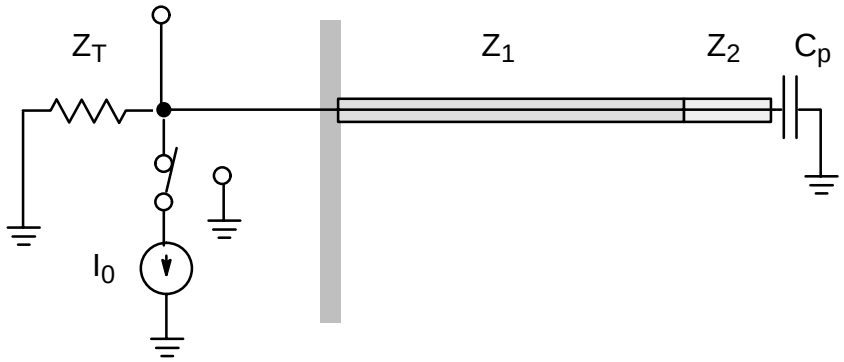

Fig. 5.3: The schematic of the time domain reflectometry measurement of a cable and a button with feedthrough. When t < 0, the switch at the current source is closed. At t = 0, the switch opens and the propagation of the voltage change begins to propagate to the right.

We apply the results obtained in Section 5.1, with the boundary conditions

$$V(0,t) = -Z_T I(0,t) \tag{5.25}$$

and

$$I(l_1 + l_2, t) = C_p \frac{\partial V}{\partial t}(l_1 + l_2, t). \tag{5.26}$$

l_1 and l_2 are the lengths of the connecting cable and the button feedthrough, respectively. Taking the Laplace transform of Eqs. (5.25) and (5.26), we have

$$\tilde{V}(0,s) = -Z_T \tilde{I}(0,s), \tag{5.27}$$

$$\tilde{I}(1_1 + 1_2, s) = C_p\left\{s\tilde{V}(l_1 + 1_2, s) + I_0 Z_T\right\}. \tag{5.28}$$

Here, the initial voltage V_0 was set at $-I_0Z_T$. The coefficients A_1, B_1, A_2, and B_2 in Eqs. (5.7) and (5.8) can be obtained using Eqs. (5.10), (5.27), and (5.28). The result is

$$A_1 = \frac{I_0 Z_T Z_1}{Z_T + Z_1}\frac{1}{s\zeta(s)}\left\{1 + r_2\frac{s-\alpha}{s+\alpha}e^{-2s\Delta t_2}\right\}, \tag{5.29}$$

and

$$B_1 = -\frac{I_0 Z_T Z_1}{Z_T + Z_1}e^{-2s\Delta t_1}\frac{1}{s\zeta(s)}\left\{r_2 + \frac{s-\alpha}{s+\alpha}e^{-2s\Delta t_2}\right\}. \tag{5.30}$$

Here,

$$\zeta(s) = 1 + r_1 r_2\, e^{-2s\Delta t_1} + r_2\frac{s-\alpha}{s+\alpha}e^{-2s\Delta t_2} + r_1\frac{s-\alpha}{s+\alpha}\, e^{-2s(\Delta t_1 + \Delta t_2)}. \tag{5.31}$$

and

$$\Delta t_n = \frac{l_n}{v_n}, \quad v_n = \frac{1}{\sqrt{L_n C_n}}, \qquad (n = 1, 2) \tag{5.32}$$

$$r_1 = \frac{Z_T - Z_1}{Z_T - Z_1}, \quad r_2 = \frac{Z_1 - Z_2}{Z_1 - Z_2}, \text{ and } \quad \alpha = \frac{1}{C_p Z_2}.$$

v_1 and v_2 are the phase velocities in the cable and the button feedthrough, respectively. Now that the coefficients A_1 and B_1 have been obtained, we insert these in Eq. (5.7) and do the inverse-Laplace transform. The detected signal V(0,t) is then obtained from

$$\tilde{V}(0,s) = A_1 + B_1 - \frac{I_0 Z_T}{s}. \tag{5.33}$$

As we did in the previous section, we rewrite the coefficients A_1 and B_1 by expanding $1/\zeta(s)$ into a series. The full expression is very complicated indeed involving products of multiple powers of the terms in Eq. (5.31). In order to use approximations, we assume that the length of the cable is much longer than that of the feedthrough. We also note that we are interested only in the time interval $0 < t < 4\Delta t_1$, in which case we can truncate A_1 and B_1 at the second order of $e^{-2s\Delta t_1}$. From Eqs. (5.29), (5.30), and (5.31), we obtain

$$A_1 = \frac{I_0 Z_T Z_1}{Z_T + Z_1} + r_1 B_1, \tag{5.34}$$

and

$$B_1 = -\frac{I_0 Z_T Z_1}{Z_T + Z_1}\frac{1}{s} e^{-2s\Delta t_1}\left[r_2 + (1 - r_{2^2})\sum_{n=1}^{N-1}(-r_2)^{n-1} e^{-2ns\Delta t_2}\left(\frac{s-\alpha}{s+\alpha}\right)^n\right]. \tag{5.35}$$

$N = \dfrac{\Delta t_1}{\Delta t_2}$ is a large number. The expressions for A_1 and B_1 in Eqs. (5.34) and (5.35) are good only in the time interval $0 < t < 4\Delta t_1$. From Eq. (5.33) we obtain

$$\tilde{V}(0,s) = \frac{Z_T}{Z_T + Z_1}\left(2B_1 - \frac{I_0 Z_T}{s}\right). \tag{5.36}$$

In Table 5.1 are listed functions $u_n(t)$, the inverse-Laplace transforms of $\frac{1}{s}\left(\frac{s-\alpha}{s+\alpha}\right)^n$. Since r_2 is typically very small, the series in Eq. (5.35) converges very rapidly and only a few terms are sufficient for our purpose.

n	$u_n(t)$, $t > 0$
0	0
1	$-1 + 2^{-\alpha t}$
2	$1 - 4\alpha t\, e^{-\alpha t}$
3	$-1 + e^{-\alpha t}(2 - 4\alpha t + 4\alpha^2 t^2)$
4	$1 - e^{-\alpha t}\left(8\alpha t = 8\alpha^2 t^2 + \frac{8\alpha^3 t^3}{3}\right)$
5	$-1 + e^{-\alpha t}\left(2 - 8\alpha t + 16\alpha^2 t^2 - 8\alpha^3 t^3 + \frac{4\alpha^4 t^4}{3}\right)$
6	$1 - e^{-\alpha t}\left(12\alpha t - 24\alpha^2 t^2 + \frac{56\alpha^3 t^3}{3} - \frac{16\alpha^4 t^4}{3} + \frac{8\alpha^5 t^5}{15}\right)$

Table 5.1: Inverse-Laplace transform of $\frac{1}{s}\left(\frac{s-\alpha}{s+\alpha}\right)^n$.

In terms of the functions $u_n(t)$ listed in Table 5.1, V(0,t) can be written as

$$V(0,t) = -\frac{I_0 Z_{T^2}}{Z_T + Z_1}\left[u_0(t) + \frac{2Z_1}{Z_T + Z_1}\left\{r_2\, u_0(t - 2\Delta t_1) + (1 - r_{2^2})\sum_{n=1}^{N-1}(-r_2)^{n-1} u_n(t - 2\Delta t_1 - 2n\Delta t_2)\right\}\right]. \tag{5.37}$$

Equation (5.37) is the expression for the detected signal at the acquisition point for $0 < t < 4\Delta t_2$. As an example, take

$$l_1 = 30 \text{ cm}, l_2 = 1 \text{ cm}, r_1 = 0.1, r_2 = -0.1,$$

$$I_0 = 10 \text{ mA}, Z_T = 50\ \Omega,$$

$$v_1 = v_2 = 20 \text{ cm/nsec},$$

$$\alpha = 1/C_p Z_2 = 1/(5\times10^{-12}\times50)\ \text{sec}^{-1} = 4 \text{ /nsec}.$$

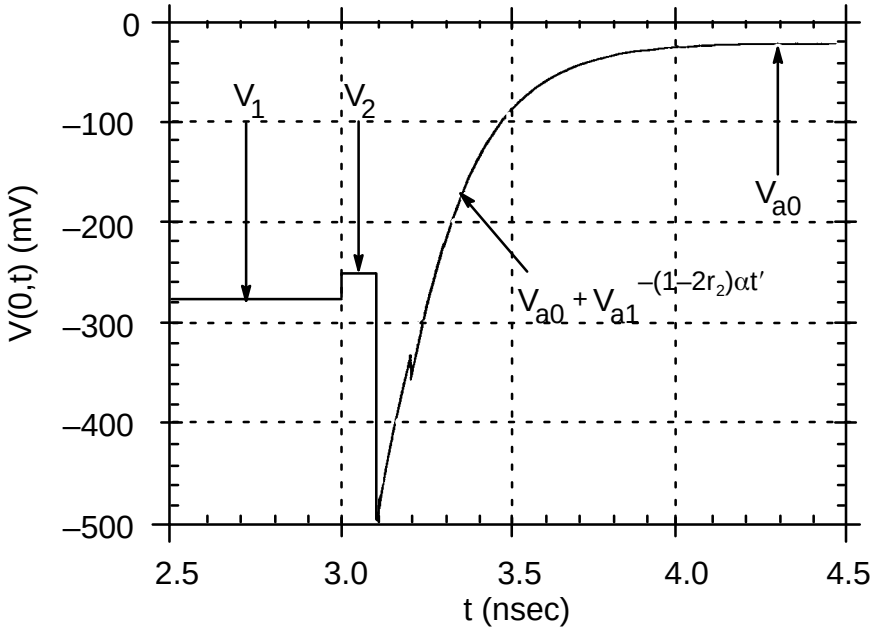

Fig. 5.4: Theoretically derived TDR trace of a button connected to a cable. The constants V_1, V_2, V_{a0}, and V_{a1} are given in Eqs. (5.38), (5.39), (5.41), and (5.42), respectively.

The plotting of V(0,t) is shown in Fig. 5.4. The several discontinuities are due to the standing wave caused by the impedance mismatch among the terminating resistor, the cable, and the button feedthrough. These may not show in the actual measurement because of the finite bandwidth of detection. The initial flat signal given by

$$V_1 = -\frac{I_0 Z_{T^2}}{Z_T + Z_1} \tag{5.38}$$

corresponds to the propagation through the cable plus the reflection at the boundary between the cable and the feedthrough. The time duration is twice the length of the cable. The second flat signal given by

$$V_2 = \frac{I_0 Z_{T^2}}{Z_T + Z_1}\left\{1 + \frac{2Z_1(Z_1 - Z_2)}{(Z_T + Z_1)(Z_1 + Z_2)}\right\} \tag{5.39}$$

is the propagation through the button feedthrough. This is again reflected at the button electrode. The subsequent rise and exponential decay due to the button capacitance is intermittently interrupted by the standing wave in the feedthrough, as shown by the discontinuities in the signal. In

order to use this curve to estimate the button capacitance, these discontinuities must be smeared out by averaging, which is partly done by the filtering due to the finite bandwidth of the instrument. The finite bandwidth also introduces bumps at the transitions between the cable, the feedthrough, and the electrode. (In the real measurement, the voltage signal exhibits oscillations for a long time as shown in Fig. 5.6(b), and further smoothing and fitting is necessary.) In the limit $\Delta t_2 << \Delta t_1$ and to the first order of r_1 and r_2, the voltage $V_a(t > 2(\Delta t_1 + \Delta t_2))$ is given by

$$V_a)t' \approx V_{a0} + V_{a1} e^{-(1-2r_2)\alpha t'}, \tag{5.40}$$

where t' = t – 2(Δt_1 + Δt_2). The constants V_{a0} and V_{a1} are given by

$$V_{a0} = -\frac{I_0 Z_{T^2}(Z_T - Z_1)}{(Z_T + Z_1)^2}, \tag{5.41}$$

and

$$V_{a1} = -\frac{4I_0 Z_{T_2} Z_1)}{(Z_T + Z_1)^2} \tag{5.42}$$

In Eq. (5.40), substitution was made for $1 + 2r_2\alpha t' \rightarrow e^{2r_2\alpha t'}$. The time constant of decay is

$$\tau = \frac{1}{\alpha(1 - 2r_2)} = C_p\left\{Z_1 + \frac{(Z_1 + Z_2)^2}{3Z_2 - Z_1}\right\} \approx C_p Z_1. \tag{5.43}$$

The second term in Eq. (5.43) was dropped in the last step, since it is of the second order in r_2. From Eq. (5.43), the button capacitance can be estimated by measuring the decay time constant and the characteristic impedance of the cable.

5.4 Measurement

In this section, we will give an example of measuring the characteristic impedance of the cable, the button feedthrough, and the button capacitance using TDR. Figures 5.5 and 5.6 show the measured TDR traces of a button and a cable. The button is one of those to be installed in the APS storage ring and has a female type SMA connector. From Fig. 5.4, the initial voltage $V_0 = -I_0 Z_T$ was measured to be –499.38 mV. Since I_0 and Z_T cannot be measured separately, we set I_0 = 9.988 mA and Z_T = 50 Ω. The error due to this uncertainty is 0.12%.

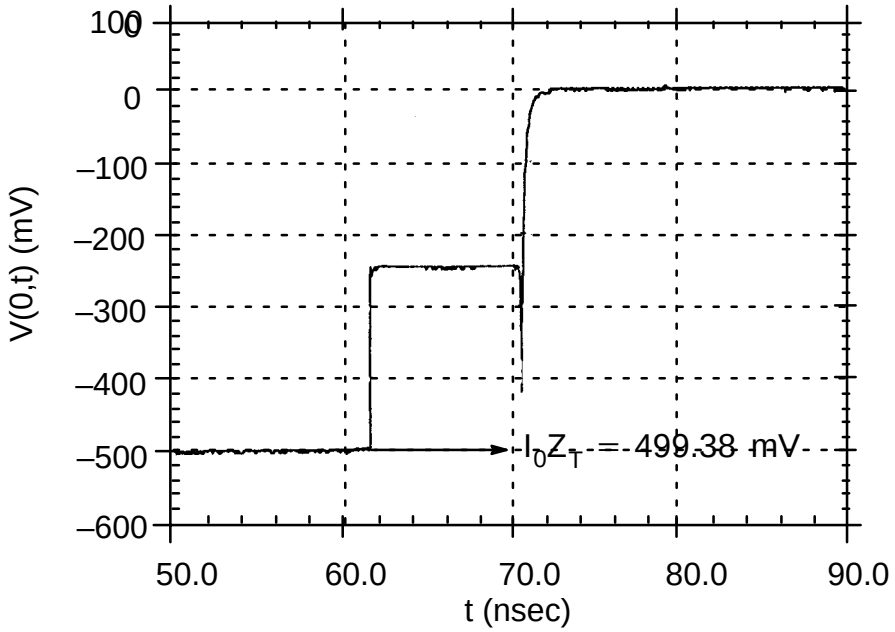

Fig. 5.5: Measured TDR trace of a cable and a button. The switch at the current source was opened at t = 61.7 nsec. The initial voltage $V_0 = -I_0Z_T$ is –499.38 mV.

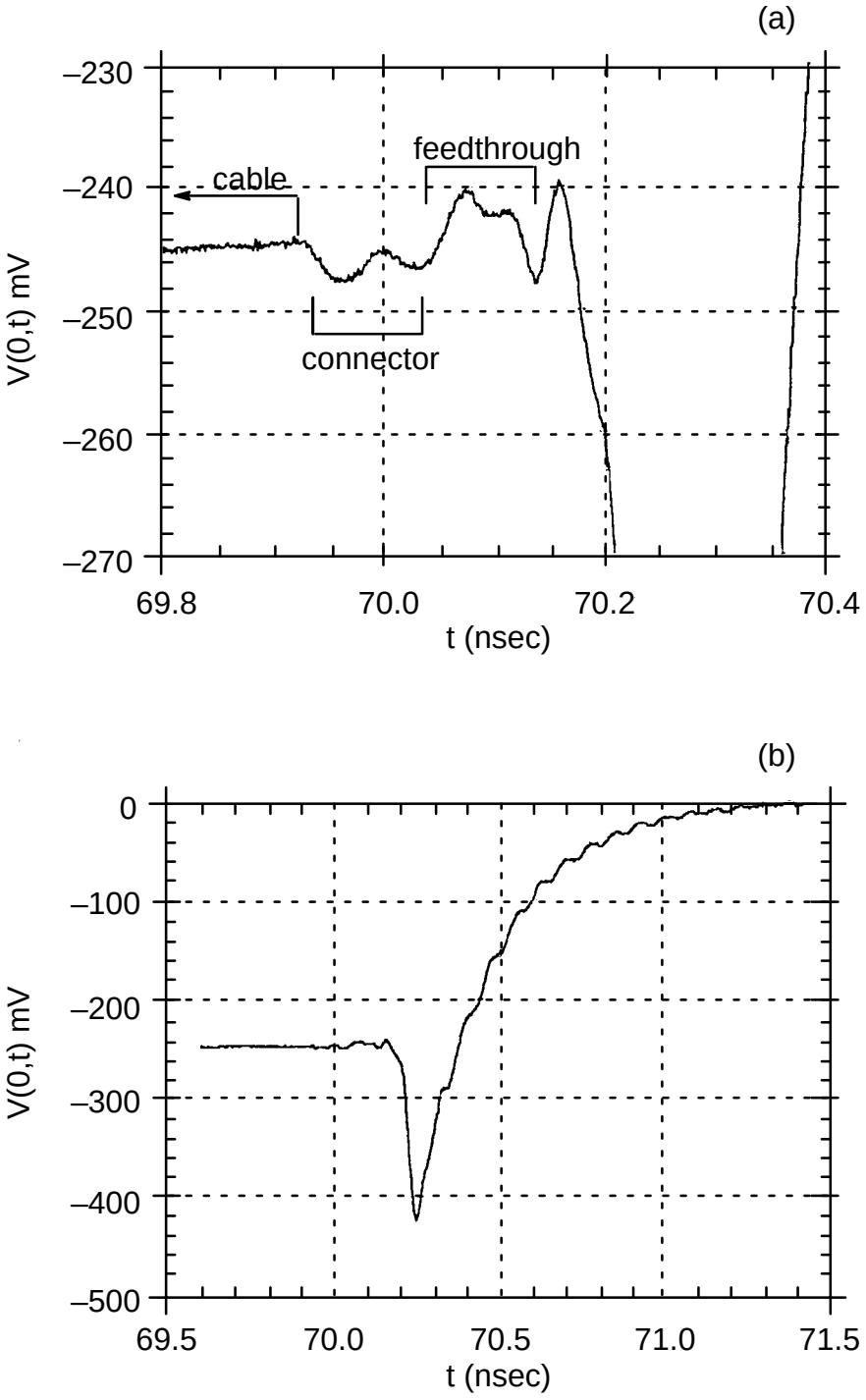

Fig. 5.6: Measured TDR trace of a cable and a button. (a) is the magnified view of the transition between the cable and the feedthrough at t ≈ 70.0 nsec. (b) shows exponential decay of the signal. The slight oscillation is due to imperfections in the junctions, e.g., the connectors and the gap between the electrode and the feedthrough.

The trace in Fig. 5.6(a) shows the transition between the cable and the feedthrough The two bumps at t ≈ 70 ns is due to the connector on the cable. The characteristic impedance Z_1 of

the cable is read from the straight line before 70 nsec, and the characteristic impedance Z_2 of the feedthrough is read from the plateau at $t \approx 70.1$ nsec. Using Eqs. (5.38) and (5.39), the measured characteristic impedances are $Z_1 = 51.94\ \Omega$ and $Z_2 = 53.04\ \Omega$.

The exponential decay due to the button capacitance is shown in Fig. 5.6(b). The oscillation superimposed on the exponential decay has approximately 13 GHz frequency (T = 77 psec). The measured time constant of decay τ is 0.262 nsec, and using Eq. (5.43), the capacitance is C_p = 5.04 pF.

6. Application of Lambertson's Method for Offset Calibration

Let V_m be the voltage applied at the m-th button and let V_n be the voltage measured at the n-th button as shown in Fig. 6.1. Then the normalized signal V_{nm} is given by[1]

$$V_{nm} = \frac{V_n}{V_m} = 2\ Z_T\, g_n\ G_{nm}\ g_m. \tag{6.1}$$

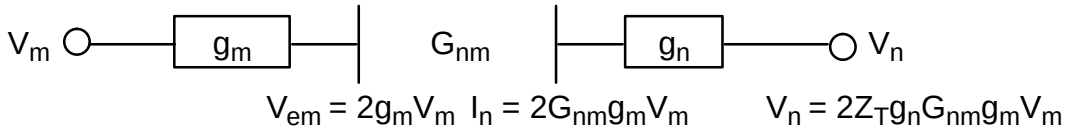

Fig. 6.1: The coupling between the buttons n and m.

G_{nm} is the capacitive coupling constant between buttons, and the gain coefficients g_n are given by Eq. (4.9). Note that V_{nm} is a symmetric matrix. With four buttons, up to 12 measurements of V_{nm} may be made and the gain coefficients are expressed in terms of V_{nm} and G_{nm} as shown in Eq. (6.2). With these gain coefficients associated with the buttons (see Fig. 6.2), the electrical center relative to the mechanical center of the BPM can be determined.

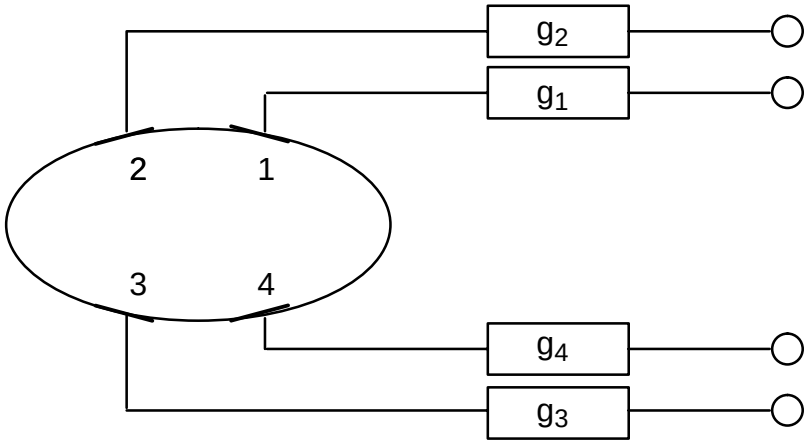

Fig. 6.2: The schematic of the button configuration. g's represent the gain associated with the buttons.

$$\begin{aligned}
2\cdot Z_T\cdot g_{1^2} &= \frac{V_{21}V_{14}}{V_{42}}\frac{G_{13}}{G_{12}G_{23}} = \frac{V_{12}V_{31}}{V_{32}}\frac{G_{23}}{G_{12}G_{13}} = \frac{V_{41}V_{31}}{V_{43}}\frac{G_{12}}{G_{23}G_{13}},\\
2\cdot Z_T\cdot g_{2^2} &= \frac{V_{21}V_{32}}{V_{31}}\frac{G_{13}}{G_{12}G_{23}} = \frac{V_{21}V_{42}}{V_{14}}\frac{G_{23}}{G_{12}G_{13}} = \frac{V_{32}V_{42}}{V_{43}}\frac{G_{12}}{G_{23}G_{13}},\\
2\cdot Z_T\cdot g_{3^2} &= \frac{V_{32}V_{43}}{V_{42}}\frac{G_{13}}{G_{12}G_{23}} = \frac{V_{43}V_{31}}{V_{14}}\frac{G_{23}}{G_{12}G_{13}} = \frac{V_{32}V_{31}}{V_{21}}\frac{G_{12}}{G_{23}G_{13}},
\end{aligned} \tag{6.2}$$

$$2\cdot Z_T\cdot g_{4^2} = \frac{V_{43}V_{14}}{V_{31}}\frac{G_{13}}{G_{12}G_{23}} = \frac{V_{43}V_{42}}{V_{32}}\frac{G_{23}}{G_{12}G_{13}} = \frac{V_{14}V_{42}}{V_{21}}\frac{G_{12}}{G_{23}G_{13}},$$

If we assume 2-D symmetry of the button configuration, that is, $G_{12} = G_{34}$, $G_{14} = G_{23}$, and $G_{13} = G_{24}$, the gain factors can then be obtained from three alternative combinations of the measured V_{nm} as shown in Eq. (6.1). Since we are interested in the ratios of the gain factors, the values of G's need not be known.

7. Nullification of Offset by Matching

From Eq. (4.9) the gain coefficient g_e is a function of S_{11}, S_{12} (or S_{21}) and C_p, and from Eqs. (3.3) and (3.4), S parameters are again functions of the characteristic impedance and the cable length. These parameters can be measured using TDR as described in Section 5, or alternatively using a network analyzer. Once the measurements of the capacitance C_p and the characteristic impedance Z_p on buttons and the characteristic impedance Z_c and the cable length L_c are done on a large number (≈ 2,000) of buttons and cables, the buttons will be sorted in fours with closely matching C_p and Z_p, and the cables will be sorted likewise. The characteristic impedances Z_p and Z_c need not be matched. This way, the gain coefficients g_e can be made uniform among the four buttons and extra offset calibration may not be necessary.

8. Summary

In this note, a basic theory of wave propagation in dielectric media was discussed in conjunction with S parameters to derive the button gain coefficients g_e and an analytic expression for the signal from TDR measurement on a cable and a button. These formulas in Eqs. (4.9), (5.38), (5.39), and (5.43) can be used to measure the button capacitance and the characteristic impedances of the cable and the button feedthrough. S parameters can again be written in terms of the characteristic impedance and the length of the cable as in Eqs. (3.3) and (3.4).

Since g_e is a function of S parameters (S_{11} and S_{12}) and the button capacitance C_p, it is possible to make the gain coefficients the same for all four buttons in a BPM by carefully matching the buttons and the cables.

Appendix A. S parameters of combined devices**.**

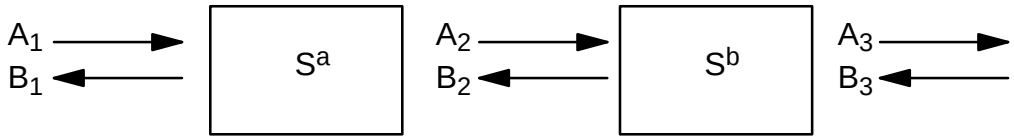

Fig. A.1: Two devices with S parameters S^a and S^b connected in series.

Consider two devices with S parameters S^a and S^b as shown in Fig. A.1. We want to obtain the S parameter of the combined system as a function S^a and S^b. This new S parameter relates A_1, B_1, A_3 and B_3. Let A_2 and B_2 be the amplitudes of the forward-traveling and the backward traveling wave between the devices a and b. Then we have

$$\begin{pmatrix} B_1 \\ A_2 \end{pmatrix} = S^a \begin{pmatrix} A_1 \\ B_2 \end{pmatrix} \text{ and } \begin{pmatrix} B_2 \\ A_3 \end{pmatrix} = S^b \begin{pmatrix} A_2 \\ B_3 \end{pmatrix}. \qquad (A.1)$$

Eliminating A_2 and B_2 from Eq. (A.1), we obtain

$$B_1 = \left[S^{a}_{11} + \frac{S^{a}_{12} S^{a}_{21} S^{b}_{11}}{1 - S^{a}_{22} S^{b}_{11}} \right] A_1 + \frac{S^{a}_{12} S^{b}_{12}}{1 - S^{a}_{22} S^{b}_{11}} B_{3,} \tag{A.2}$$

$$A_3 = \frac{S^{a}_{21} S^{b}_{21}}{1 - S^{a}_{22} S^{b}_{11}} A_1 + \left[S^{b}_{22} + \frac{S^{a}_{22} S^{b}_{21} S^{b}_{12}}{1 - S^{a}_{22} S^{b}_{11}} \right] B_3.$$

This gives Eqs. (3.5) to (3.8).

Appendix B. Solution of $\frac{\partial^2\tilde{V}}{\partial z^2} - h^2\tilde{V} = -\frac{h^2}{s}V(z,0)$.

In this appendix, we obtain the solution of Eq. (5.6),

$$\frac{\partial^2\tilde{V}}{\partial z^2} - h^2\tilde{V} = -\frac{h^2}{s}V(z,0), \tag{B.1}$$

where $h = s\sqrt{LC}$. The homogeneous solution $\tilde{V}_h$ is easily obtained as

$$\tilde{V}(z,s) = A\ e^{-hz} + Be^{hz}. \tag{B.2}$$

A and B are arbitrary constants. To obtain the particular solution $\tilde{V}_p$, we will use the Green's function method. Let G(z,z′) be the Green's function which satisfies

$$\frac{\partial^2 G(z,z')}{\partial z^2} - h^2 G(z,z') = \partial(z - z'). \tag{B.3}$$

Then $\tilde{V}_p$ is written as

$$\tilde{V}_p = \frac{h^2}{s}\int_{-\infty}^{\infty} dz'\ G(z,z')V(z',0). \tag{B.4}$$

Now, write

$$G(z,z') = \begin{cases} c_1\ e^{-h(z-z_0)} + d_1\ e^{h(z-z_0)}, & z > z' \\ c_2\ e^{-h(z-z_0)} + d_2\ e^{h(z-z_0)}, & z > z' \end{cases} \tag{B.5}$$

Since G(z,z′) should converge as $z \to \pm\infty$, we have $c_2 = d_1 = 0$. The continuity condition at $z = z'$ gives $c_1 = d_2$. Integrating Eq. (B.3) from z′–δ and z′+δ (δ→0), we obtain

$$\left(\frac{\partial G(z,z')}{\partial z}\right)_{z=z'+\delta} - \left(\frac{\partial G(z,z')}{\partial z}\right)_{z=z'-\delta} = 1, \tag{B.6}$$

which gives

$$c_1 = d_2 = -\frac{1}{2h}. \tag{B.7}$$

From Eqs. (B.5) and (B.7), we have

$$G(z,z') = -\frac{1}{2h}e^{h|z-z'|} \tag{B.8}$$

and from Eq. (B.4), we obtain

$$\tilde{V}_p = \frac{h}{2s}\int_{-\infty}^{\infty} dz'\ e^{h|z-z'|}V(z',0). \tag{B.9}$$

The complete solution $\tilde{V} = \tilde{V}_h + \tilde{V}_p$ is then, combining Eqs. (B.2) and (B.9),

$$\tilde{V} = A\ e^{-hz} + B\ e^{hz} + \frac{h}{2s}\int_{-\infty}^{\infty} dz'\ e^{h|z-z'|}V(z'0) \tag{B.10}$$

Acknowledgment

G. Decker is to be thanked for his support and stimulating discussions.

References

1. G. R. Lambertson, “Calibration of Position Electrodes Using External Measurements”, LSAP Note-5, Lawrence Berkeley Laboratory, May 6, 1987
2. J. Hinkson, private communication.
3. G. Decker, Y. Chung and E. Kahana, “Progress on the Development of APS Beam Position Monitoring System”, Proceedings of 1991 IEEE Particle Accelerator Conference.
4. Y. Chung and G. Decker, “Offset Calibration of the Beam Position Monitor Using External Means”, Proceedings of 1991 Accelerator Instrumentation Workshop.
5. J. Stratton, *Electromagnetic Theory* , MacGraw Hill, p. 283, 1941.
6. J. Slater, *Microwave Electronics* , D. van Nostrand, Chapter II, 1950.